Geostrophic eddies, abyssal recirculations, and zonal jets

David P. Marshall, Susan T. Adcock, and Claire E. Tansley

Department of Meteorology, University of Reading, Reading, United Kingdom

Abstract. A characteristic property of geostrophic turbulence is that energy undergoes an inverse cascade to large spatial scales, whereas potential enstrophy cascades directly to small spatial scales. In the presence of weak dissipation, such as in the ocean, energy is therefore quasi-conserved whereas potential enstrophy is always dissipated. As a consequence geostrophic eddies only partially mix potential vorticity along isopycnals, with the amount of mixing being dependent on the energy available in the initial state. To illustrate these ideas, two oceanographic applications are considered: the generation of abyssal recirculations around topographic features and the formation of inertial zonal jets. A new eddy parameterization is developed that dissipates potential enstrophy subject to the constraint of conserving energy. Results obtained using the parameterization are compared with those from an eddy-resolving calculation. Possible extensions of these ideas are discussed, including the possibility of incorporating additional constraints such as conservation of angular momentum.

Introduction

The ocean contains an intense geostrophic eddy field, with a dominant energy-containing scale of order 100 km at midlatitudes. In order to obtain plausible turbulent cascades of dynamic and passive tracers it is necessary for models to resolve even finer spatial scales of order 10 km (e.g., *Roberts and Marshall*, 1998), and consequently ocean climate models are unlikely to adequately resolve the geostrophic eddy field for several years. Development of parameterizations of unresolved geostrophic turbulent processes therefore remains an important task for ocean modelling and climate prediction. But at least as importantly, development of parameterizations is also an excellent strategy for testing and further advancing our understanding of geostrophic turbulence and its impact on the large-scale circulation.

The performance of numerical ocean models has recently been transformed by the widespread adoption of the *Gent and McWilliams* (1990) parameterization (hereafter GM). The key idea behind their parameterization is that geostrophic eddies adiabatically rearrange fluid parcels along isopycnals, without changing the density of individual fluid parcels. Consequently GM represents the eddy flux of a passive tracer through both a diffusion along isopycnals and an advection by an "eddy-induced transport velocity" (*Gent et al.*, 1995). These adiabatic conservations properties have led to a series of dramatic improvements in ocean models, including improved global temperature distribution, improved poleward and surface heat fluxes, and improved occurrence of deep convection (*Danabasoglu et al.*, 1994).

Nevertheless there remain significant shortcomings of GM. For example, the eddy-induced transport in GM is chosen to mimic the effects of baroclinic instability by extracting potential energy from the mean flow, thus driving the ocean towards a state of rest with flat isopycnals. In contrast a number of studies suggest that under appropriate conditions, geostrophic eddies can homogenize the potential vorticity field along isopycnals (*Holland and Rhines*, 1980; *Rhines and Young*, 1982; *Marshall et al.*, 1999). These results have led to alternative closures for the eddy-induced transport in terms of isopycnic gradients of potential vorticity (*Treguier et al.*, 1997; *Killworth*, 1997). However other studies suggest that while eddies may mix potential vorticity along isopycnals, the potential vorticity field is not necessarily homogenized (e.g., *Bretherton and Haidvogel*, 1976; *Wang and Vallis*, 1994).

In this paper we review two oceanographic phenomena in which eddies mix the potential vorticity field along isopycnals without making the potential vorticity uniform. Firstly we consider the formation of anticy-

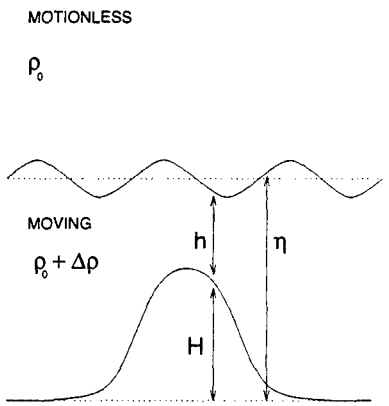

Figure 1. The inverted shallow water model. Motion is confined to a dynamically active abyssal layer, thickness h, overlying variable bottom topography, height H. The height of the layer inteface is $\eta = H + h$. (From *Adcock and Marshall*, 2000.)

clonic recirculations around topographic features (also known as "cold domes"). We diagnose the nature of the turbulent cascades in the formation of such recirculations, based on which we develop a new energy-conserving eddy parameterization. Secondly we consider the formation of inertial zonal jets embedded within a larger-scale flow. Finally we discuss some possible extensions and wider implications of our results.

Abyssal recirculations

In this section we review the results of some numerical experiments illustrating the interactions between geostrophic eddies and the mean circulation in the presence of variable bottom topography (*Adcock and Marshall*, 2000). The experiments are performed using an "inverted" shallow-water model, in which motion is confined to a dynamically active abyssal layer, thickness h, overlying variable bottom topography, height H (Figure 1). While highly idealized, this model captures the following key ingredients: a geostrophic eddy field, a Rossby deformation radius, a variable isopycnal interface, and variable bottom topography. In these experiments, we simply initialize with an ensemble of balanced geostrophic eddies and integrate forwards in time for 40 model years.

The equations of motion can be written:

$$\frac{\partial u}{\partial t} + u\frac{\partial u}{\partial x} + v\frac{\partial u}{\partial y} - fv + g'\frac{\partial \eta}{\partial x} = -A\nabla^4 u, \quad (1)$$

$$\frac{\partial v}{\partial t} + u\frac{\partial v}{\partial x} + v\frac{\partial v}{\partial y} + fu + g'\frac{\partial \eta}{\partial y} = -A\nabla^4 v, \quad (2)$$

$$\frac{\partial h}{\partial t} + \frac{\partial}{\partial x}(hu) + \frac{\partial}{\partial y}(hv) = 0. \quad (3)$$

Here $\eta = h + H$ is the height of the layer interface, u, v are the velocity components in the x, y directions respectively, $f = f_0 + \beta y$ is the Coriolis parameter where $f_0 = 0.7 \times 10^{-4}\mathrm{s}^{-1}$ and $\beta = 2 \times 10^{-11}\mathrm{m}^{-1}\mathrm{s}^{-1}$, and $g' = 0.02\,\mathrm{m\,s}^{-2}$ is the reduced gravity. We solve in a square domain (dimension 1000 km) containing a seamount of height 500 m. The mean value of η is 750 m. A scale-selective biharmonic dissipation is employed in the momentum equations to dissipate preferentially at the grid 'lscale; in our reference experiment we employ a dissipation coefficient of $A = 2.5 \times 10^8\mathrm{m}^4\mathrm{s}^{-1}$. The equations are discretized on a C-grid with a grid spacing of 5 km. Further details can be found in *Adcock and Marshall* (2000).

Figure 2 shows the evolution of the interface height (equivalent to streamlines for the geostrophic flow). The initial interface height field reveals a series of geostrophic eddies with maximum geostrophic velocities of order $30\,\mathrm{cm\,s}^{-1}$. After 4 months there is the first indication of the interface rising over the seamount. After 5 years there is an intense "cold dome" over the seamount and an associated anticyclonic recirculation with velocities of order $40\,\mathrm{cm\,s}^{-1}$. This intense recirculation remains even after 40 years. The amplitude of the recirculation is dependent on the amplitude of the initial eddy field. Notice that at all stages the interface height field, and thus also the energy field, remains trapped at scales comparable to, or larger than, the deformation radius.

In Figure 3 we show the equivalent snapshots of the potential vorticity field,

$$Q = \frac{f + \zeta}{h}, \quad (4)$$

where $\zeta = \partial v/\partial x - \partial u/\partial y$ is the relative vorticity. At leading order, potential vorticity variations are dominated by the variations in the bottom topography, with high values of potential vorticity found over the seamount and low values found off the seamount. After 4 months there is clear evidence of the direct cascade of the potential vorticity field towards small spatial scales with filaments of high potential vorticity moving off the seamount and filaments of low potential vorticity moving onto the seamount. After 5 and 40 years, the maximum value of the potential vorticity is significantly reduced over the seamount, but note that the potential vorticity field is not made uniform. The reduced potential vorticity is associated with increased layer thickness over the seamount, and hence the cold doming and the anticyclonic circulation. In contrast, a uniform potential vorticity state would require a far

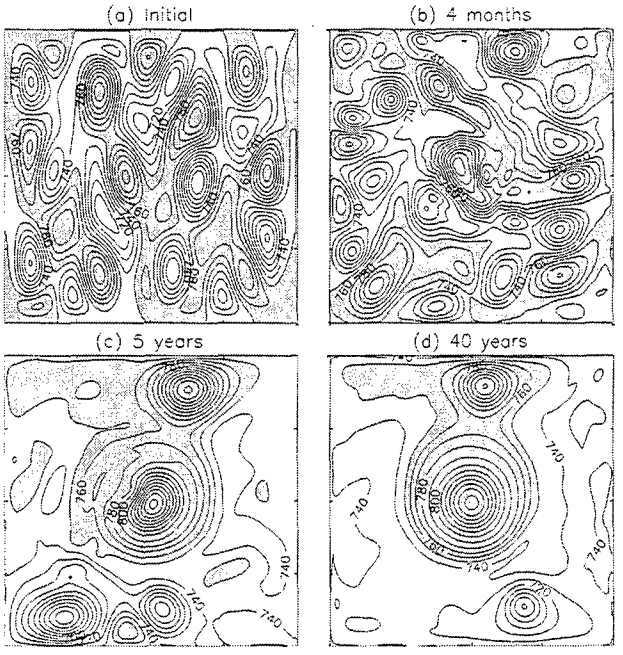

Figure 2. Interface height, η (shading indicates values greater than 750 m). (a) Initial conditions; (b) after 3 months; (c) after 5 years; (d) after 40 years. Contour interval=10m. (From *Adcock and Marshall*, 2000.)

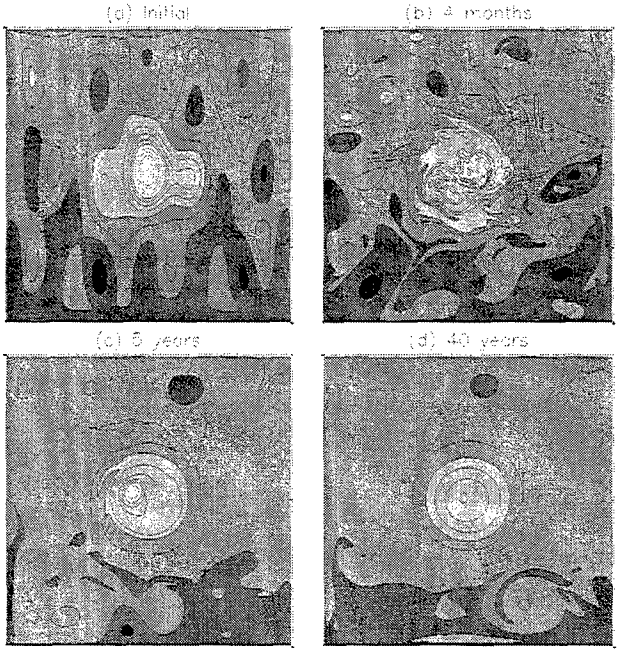

Figure 3. Potential vorticity in the abyssal layer. (a) Initial conditions; (b) after 3 months; (c) after 5 years; (d) after 40 years. Contour interval=$2 \times 10^{-8}\mathrm{m}^{-1}\mathrm{s}^{-1}$. (From *Adcock and Marshall*, 2000.)

greater doming of the layer interface over the seamount, which is impossible without an input of energy.

More quantitatively we can consider the evolution of the net available energy

$$E = \rho_o \int\int \left\{ \frac{h(u^2+v^2)}{2} + \frac{g'h(h+2H)}{2} \right\} dx\, dy, \quad (5)$$

and the net potential enstrophy,

$$\Lambda = \int\int \frac{hQ^2}{2}\, dx\, dy, \quad (6)$$

the latter being a measure of the variance of the potential vorticity field and thus the extent to which the potential vorticity field is mixed. Figure 4(a) shows the available energy over the first five model years for different values of biharmonic momentum dissipation. The amount of energy dissipated increases with the coefficient of momentum dissipation, but in each case the energy dissipated is small compared with the energy that would be dissipated if the eddies were spinning the ocean down towards a state of rest. Figure 4(b) shows the potential enstrophy over the same period. The potential enstrophy rapidly decreases below the level consistent with spin-down towards a state of rest, but similarly never approaches the level consistent with a state of uniform potential vorticity. The evolution of the potential enstrophy is remarkably insensitive to the level of momentum dissipation. These results suggest that eddies are neither driving the model ocean down towards a state of rest, as assumed in GM, nor towards a state of uniform potential vorticity. Instead the ocean is driven towards a state of minimum potential enstrophy, subject to the constraint of (nearly) conserving the net available energy (c.f. *Bretherton and Haidvogel*, 1976).

An energy-conserving parameterization

The above results can be exploited to develop a new geostrophic eddy parameterization. As in GM we represent the eddies through a rearrangement of fluid parcels or "eddy-induced transport", $\mathbf{U}^*$, such that the continuity equation becomes

$$\frac{\partial h}{\partial t} + \nabla.(h\mathbf{u} + \mathbf{U}^*) = 0. \quad (7)$$

We write the eddy-induced transport in the form

$$\mathbf{U}^* = U_o\, \mathbf{a}, \quad (8)$$

where

$$\frac{\int\int \mathbf{a}.\mathbf{a}\, dx\, dy}{\int\int dx\, dy} = 1. \quad (9)$$

Here U_0 is taken as an externally prescribed parameter controlling the *rate* at which rearrangements occur,

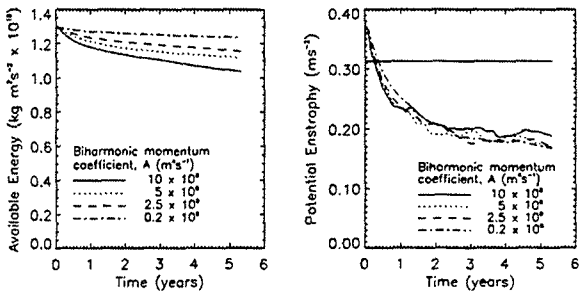

Figure 4. Evolution of (a) the total available energy and (b) the total available potential enstrophy over the first five years. The four curves correspond to different coefficients of biharmonic momentum dissipation. The thick solid line in (a) corresponds to the energy of the minimum energy state in which the ocean is at rest. The upper thick line in (b) corresponds to the potential enstrophy of the minimum energy state and the lower thick line corresponds to the potential enstrophy of the uniform potential vorticity state. (From *Adcock and Marshall*, 2000.)

while $\mathbf{a}$ describes the *spatial pattern* of these rearrangements.

We now seek the form of $\mathbf{a}$ that, in a given time interval Δt, *maximizes* the dissipation of potential enstrophy,

$$-\Delta\Lambda = \Delta t \iint \mathbf{U}^*.\nabla\frac{Q^2}{2}\,dx\,dy. \tag{10}$$

subject to conserving the total available energy,

$$\Delta E = \Delta t \iint \mathbf{U}^*.\nabla B\,dx\,dy = 0, \tag{11}$$

where $B = g'\eta + (u^2+v^2)/2$ is the Bernoulli potential. Taking variations, $\delta\mathbf{a}$, in order to maximize (10), subject to the constraints (9) and (11), gives

$$\mathbf{U}^* = \kappa\left(\nabla\frac{Q^2}{2} + \lambda\nabla B\right). \tag{12}$$

Here κ is a Lagrange multiplier determined uniquely by (9), and λ is a Lagrange multiplier determined uniquely by the energy constraint (11).

The first term in (12) corresponds to a potential vorticity closure for $\mathbf{U}^*$, whereas to leading order the second term corresponds to the GM closure. The new parameterization thus contains elements of both the GM and potential vorticity closures, and results in partial, but not total, mixing of potential vorticity.

To illustrate the use of the parameterization, in Figure 5 we show the results of three parallel simulations, the first at 5 km resolution with resolved geostrophic turbulence, the second at 40 km resolution and including the parameterization of the geostrophic turbulence, and the third at 40 km resolution with neither resolved nor parameterized turbulence. The integrations are initialized with the same eddy field shown in Figure 2(a). In the high-resolution case (Figure 5a, b) an intense anticyclonic recirculation is evident after 30 model weeks. The coarse resolution case with the parameterized turbulence (Figure 5c, d) is able to reproduce a plausible anticyclonic recirculation, whereas the coarse resolution case without the parameterized turbulence (Figure 5e, f) produces only a very weak recirculation. Note that the maximum value of the potential vorticity over the seamount is much higher in the latter case. While there are some differences, particularly in the details of the circulation off the seamount, we are encouraged by the ability of the parameterization to reproduce a plausible doming of the layer interface over the seamount.

Zonal jets

The formation of abyssal recirculation gyres represents a situation in which potential vorticity mixing is limited by the amount of energy available in the initial state. However even in the situation that there is a ready supply of energy, the inverse cascade of energy to large spatial scales can still restrict the extent to which potential vorticity can be mixed. This issue is a topic of ongoing research, but here we present some preliminary results that highlight some of the issues involved.

Specifically we consider eastward flow past a cylinder in a barotropic β-plane channel. The flow is maintained through a sponge layer (shaded region on the figures) within which the zonal velocity is relaxed towards a uniform value. These experiments were originally designed to study the dynamics of flow separation; further details can be found in *Tansley and Marshall* (2001), *Marshall and Tansley* (2001). Here we focus on just one aspect of these flows: the formation of zonal jets.

We solve the nondimensional barotropic vorticity equation

$$\frac{\partial\zeta}{\partial t} + \mathbf{u}.\nabla\zeta + \hat{\beta}v = \frac{1}{\mathrm{Re}}\nabla^2\zeta, \tag{13}$$

where $\zeta = \partial v/\partial x - \partial u/\partial y$ is the relative vorticity,

$$\mathrm{Re} = \frac{UL}{\nu} \tag{14}$$

is the Reynolds number, and

$$\hat{\beta} = \frac{\beta L^2}{U} = \frac{L^2}{L_R^2} \tag{15}$$

is a non-dimensional "β-parameter" or the "Rhines number"; the latter term is motivated by the "Rhines scale", $L_R = \sqrt{U/\beta}$, that controls the meridional scale of zonal jets in geostrophic turbulent flows (*Rhines*,

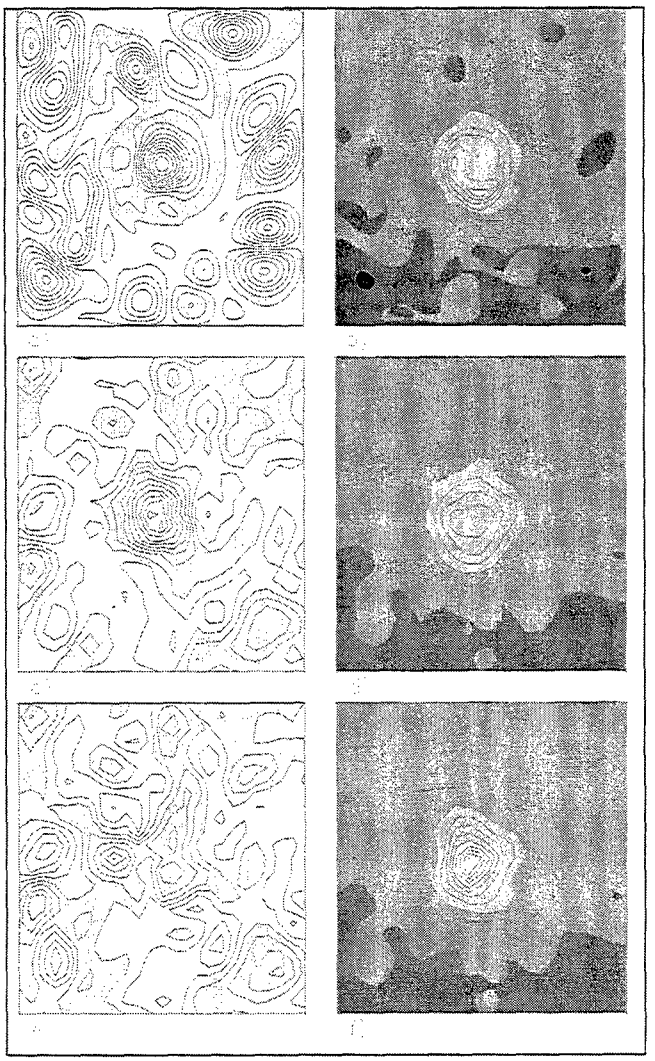

Figure 5. Snapshots of the interface height (panels a, c, e) and potential vorticity (panels b, d, f) after 30 weeks of integration. Panels a and b correspond to the 5 km resolution case with resolved turbulence; panels c and d correspond to the 40 km resolution case with the parameterization; panels e and f correspond to the 40 km resolution case without the parameterization. Contour intervals as in Figures 2 and 3. (From *Adcock and Marshall*, 2000.)

1975). Here L is the diameter of the cylinder, U is the mean zonal velocity, ν is the coefficient of lateral viscosity, and β is the gradient in the Coriolis parameter.

Here we show solutions only for the value $\hat{\beta} = 75$, and for three values of the Reynolds number. The latter controls the level of dissipation, and hence the amplitude of the eddy field. The streamfunction (ψ, defined such that $u = -\partial\psi/\partial y$, $v = \partial\psi/\partial x$) is shown in Figure 6 and the vorticity ($q = \zeta + \beta y$) is shown in Figure 7.

Even at the lowest Reynolds number of 25 (panels

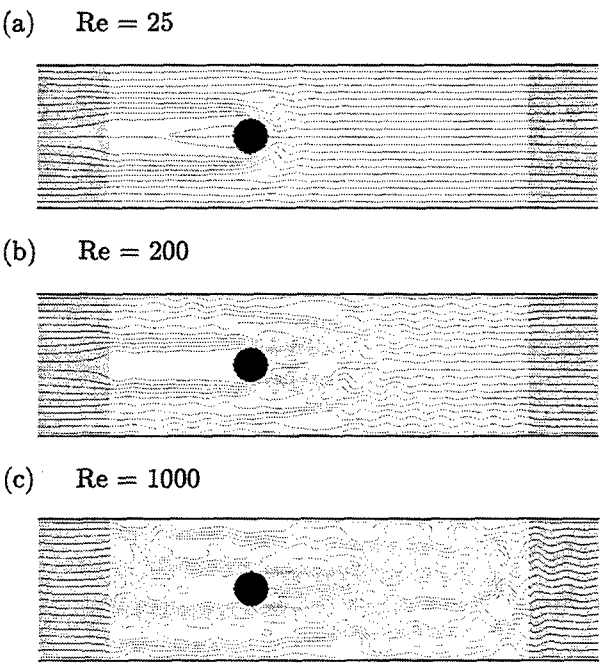

Figure 6. Streamfunction (nondimensionalized) from three solutions with $\hat{\beta} = 75$ and (a) Re = 25, (b) Re = 200, (c) Re = 1000. Contour interval = 0.2. Shading indicates the sponge layer within which the zonal velocity is relaxed towards a uniform value. (From *Tansley and Marshall*, 2001.)

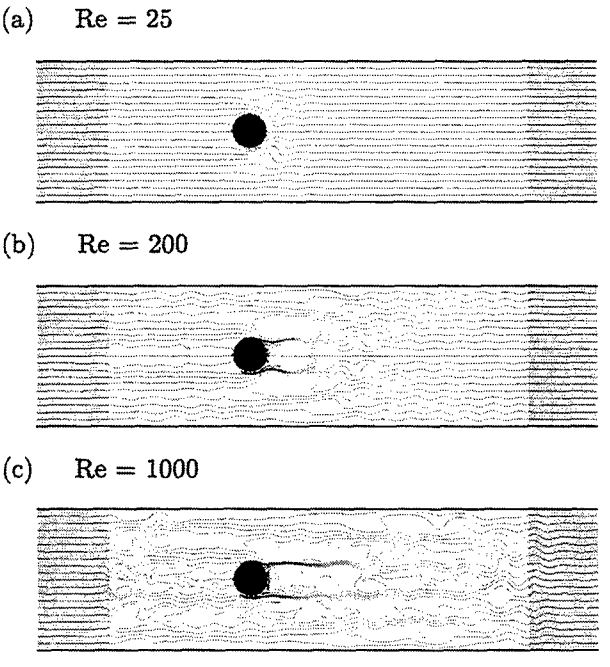

Figure 7. Vorticity (nondimensionalized) from three solutions with $\hat{\beta} = 75$ and (a) Re = 25, (b) Re = 200, (c) Re = 1000. Contour interval = 15. (From *Tansley and Marshall*, 2001.)

a), the circulation is significantly altered from the non-rotating case (not shown). Rather than a separated region downstream of the cylinder, we find a separated region upstream of the cylinder. This is related to the westward propagation of Rossby waves, and the ability of the circulation to accommodate western boundary currents, but not eastern boundary currents (e.g., see *Merkine*, 1980; *Page and Johnson*, 1990; *Tansley and Marshall*, 2001). There is a slight hint of a strongly damped Rossby wave downstream of the cylinder, but no turbulent eddies.

However at the higher Reynolds numbers of 200 (panels b) and 1000 (panels c), the circulation is fundamentally altered downstream of the cylinder. At these higher Reynolds numbers, the Rossby waves break to form a turbulent wake. Within this wake there is a direct cascade of enstrophy and an inverse cascade of energy; the latter is arrested in the meridional direction at the Rhines scale (*Rhines*, 1975), leading to the formation of a series of zonal jets. These jets extend further downstream of the cylinder at the higher value of the Reynolds number since the turbulent wake itself extends further downstream.

Just as in the formation of the abyssal recirculations, the vorticity is mixed by the eddy field, but it is not made uniform. Rather there are "plateaus" of nearly uniform vorticity, separated by narrow regions of enhanced vorticity gradient. Confirmation that the eddy field is responsible for *accelerating* the zonal jets is given in Figure 8, which shows the convergence of the eddy vorticity flux ($-\nabla.\overline{\zeta'\mathbf{u}'}$, where the overbar and primes represent time-mean and time-varying components), and the mean dissipation of vorticity through the right-hand side of (13). While the eddy term contains a rich structure, there is an unambiguous tendency to enhance the vorticity gradient across, and hence accelerate, the zonal jets. In contrast the dissipation acts to decelerate the jets.

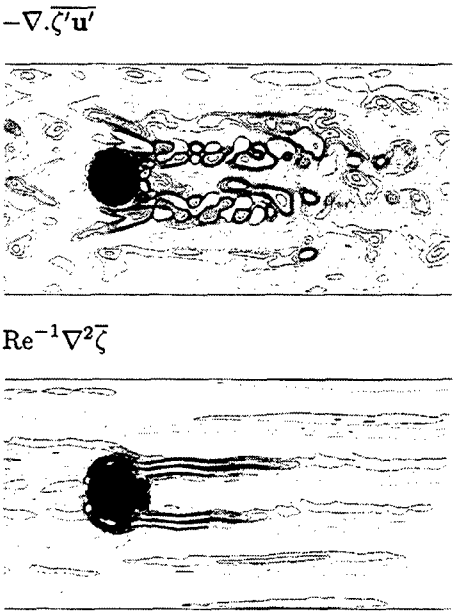

Figure 8. (a) Convergence of the eddy vorticity flux and (b) mean frictional dissipation from the solution with $\mathrm{Re} = 1000$ and $\hat{\beta} = 75$. Two contour intervals are employed: 1.0 between values of -4.5 and 4.5; and 10.0 for values of greater magnitude; shading indicates negative contours. Only the central portion of the channel is shown. (From *Tansley and Marshall*, 2001.)

Discussion

In this paper we have considered the impact of geostrophic eddies on the large-scale circulation from the perspective provided by geostrophic turbulence theory. Energy undergoes an inverse cascade to large spatial scales, whereas potential enstrophy cascades directly to small spatial scales. Consequently we argue that geostrophic eddies only partially mix potential vorticity along isopycnals, with the amount of mixing being dependent on the energy available in the initial state.

The need for an energetic constraint is clear in the formation of abyssal recirculations, since energy is required to raise isopycnals over a seamount. However we suggest that an energetic constraint might also be appropriate even in the case in which unconstrained mixing of potential vorticity leads to a net decrease in energy, since energy remains trapped at relatively large spatial scales. In Figure 9 we speculate on the implications for the slumping of a baroclinic front. According to GM, the eddy-induced transport acts to flatten the isopycnals, with a single overturning cell extending across the baroclinic front. However this slumping will result in a release of potential energy which must be converted to kinetic energy. Alternatively we suggest that the the eddy-induced transport may initially be confined to a series of localized overturning cells that act to convert available potential energy into the kinetic energy of zonal jets. This kinetic energy will in turn be dissipated through bottom drag and/or internal wave breaking, allowing further slumping to proceed. If this hypothesis is correct, then the rate at which eddies transport fluid, and tracers, across a baroclinic front should be dependent on the nature and level of dissipation in an eddy-resolving calculation. Work is in progress to explore these issues.

There is also a distinct possibility that there are additional constraints on the mixing of potential vorticity. For example in a zonal domain with no topographic variations, one should expect angular momentum to be conserved (e.g., *Marshall*, 1981). It is also unclear how

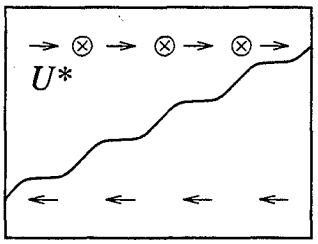

Figure 9. A hypothesis for the impact on an energetic constraint on the slumping of a baroclinic front. We suggest that the eddy-induced transport (U^*) may be confined to a series of localized overturning cells that act to convert available potential energy into the kinetic energy of zonal jets. The overall meridional transport will then depend crucially on the dissipation of the jets by bottom friction and/or internal wave breaking.

these constraints are modified in the presence of explicit forcing and dissipation, and indeed whether one should take into account the input of energy from smaller, unresolved spatial scales as suggested by *Holloway* (1987). There is also the possibility of energy transfer to small spatial scales in the presence of small-scale variations in bottom topography. These issues all require further study.

We have developed a simple energy conserving eddy parameterization in this paper. In principle it should be possible to incorporate additional constraints as required. However there are some significant limitations of our approach. In particular we apply our energy constraint in a global, rather than local, sense. The alternative approaches of *Sadournay and Basedevant* (1985) and *Holloway* (1992) may provide more practical ways forward.

Acknowledgments. DPM would like to thank Peter Müller and Chris Garrett for organizing a most stimulating and thoroughly enjoyable workshop. This work was funded by the U.K. Natural Environment Research Council.

References

Adcock, S. T., and D. P. Marshall, Interaction of geostrophic eddies and the mean circulation over large-scale bottom topography, *J. Phys. Oceanogr., 30*, 3223-3338, 2000.

Bretherton, F. P., and D. B. Haidvogel, Two-dimensional turbulence above topography, *J. Fluid Mech., 78*, 129-154, 1976.

Danabasoglu, G., J. C. McWilliams, and P. R. Gent, The role of mesoscale tracer transports in the global ocean circulation, *Science, 264*, 1123-1126, 1994.

Gent, P. R., and J. C. McWilliams, Isopycnal mixing in ocean circulation models, *J. Phys. Oceanogr., 20*, 150-155, 1990.

Gent, P. R., J. Willebrand, T. J. McDougall, and J. C. McWilliams, Parameterizing eddy-induced tracer transports in ocean circulation models, *J. Phys. Oceanogr., 25*, 463-474, 1995.

Holland, W. R., and P. B. Rhines, 1980, An example of eddy-induced ocean circulation, *J. Phys. Oceanogr., 10*, 1010-1031, 1980.

Holloway, G., Systematic forcing of large-scale geophysical flows by eddy-topography interaction, *J. Fluid Mech., 184*, 463-474, 1987.

Holloway, G., Representing topographic stress for large-scale ocean models, *J. Phys. Oceangr., 22*, 1033-1046, 1992.

Killworth, P. D., On the parameterization of eddy transfer, *J. Mar. Res., 55*, 1171-1197, 1997.

Marshall, D. P., and C. E. Tansley, An implicit formula for boundary current separation, *J. Phys. Oceanogr., 31*, 1633-1638, 2001.

Marshall, D. P., Williams, R. G., and M.-M. Lee, The relation between eddy-induced transport and isopycnal gradients of potential vorticity, *J. Phys. Oceanogr., 29*, 1571-1578, 1999.

Marshall, J. C., On the parameterization of geostrophic eddies in the ocean, *J. Phys. Oceanogr., 11*, 257-271, 1981.

Merkine, L. O., Flow separation on a β-plane, *J. Fluid Mech., 99*, 399-409, 1980.

Page, M. A., and E. R. Johnson, Flow past cylindrical obstacles on a beta-plane, *J. Fluid Mech., 221*, 349-382, 1990.

Rhines, P. B., Waves and turbulence on a beta-plane, *J. Fluid Mech., 69*, 417-433.

Rhines, P. B., and W. R. Young, Homogenization of potential vorticity in planetary gyres, *J. Fluid Mech., 122*, 347-367.

Roberts, M. J., and D. P. Marshall, Do we require adiabatic dissipation schemes in eddy-resolving ocean models? *J. Phys. Oceanogr., 28*, 1998, 2050-2063.

Sadournay, R., and C. Basedevant, Parameterization of subgrid scale barotropic and baroclinic eddies in quasi-geostrophic models: anticipated potential vorticity method, *J. Atmos. Sci., 42*, 1353-1363, 1985.

Tansley, C. E., and D. P. Marshall, Flow past a cylinder on a β-plane, with application to Gulf Stream separation and the Antarctic Circumpolar Current, *J. Phys. Oceanogr.*, 2001, in press.

Treguier, A. M., I. M. Held, and V. D. Larichev, Parameterization of quasigeostrophic eddies in primitive equation ocean models, *J. Phys. Oceanogr., 27*, 567-580, 1997.

Wang, J., and G. K. Vallis, Emergence of Fofonoff states in inviscid and viscous ocean circulation models, *J. Mar. Res., 52*, 83-127, 1994.

This preprint was prepared with AGU's LaTeX macros v4, with the extension package 'AGU++' by P. W. Daly, version 1.6a from 1999/05/21.